# Phase stability of plutonium

J. van Ek
*Department of Chemistry and Materials Science, L-268, Lawrence Livermore National Laboratory, P.O. Box 808, Livermore, California 94551*

P. A. Sterne
*Department of Physics, University of California, Davis, California 95616 and Department of Chemistry and Materials Science, L-268, Lawrence Livermore National Laboratory, P.O. Box 808, Livermore, California 94551*

A. Gonis
*Department of Chemistry and Materials Science, L-268, Lawrence Livermore National Laboratory, P.O. Box 808, Livermore, California 94551*

(Received 21 May 1993)

Results of electronic-structure calculations on the experimentally observed low-temperature monoclinic $\alpha$ phase of Pu are presented and compared to calculations for fcc ($\delta$ phase) and fictitious hexagonal Pu. Energy-volume curves for fcc and hexagonal phases of Pu reveal a tendency towards more open structures, primarily due to an increased occupation of the $6d$ band, which has a strongly itinerant character. Bonding in these structures is not dominated by the $5f$ band. However, in the experimental $\alpha$ phase, which is computed to be the most stable, the arrangement of the atoms in the unit cell is such that $5f$ bonding is strongly enhanced when compared with fcc and hexagonal Pu. In addition the $\alpha$-Pu structure benefits from a substantial charge transfer from itinerant $7s$ states to the bonding $6d$ states. A relative downward shift of the $5f$ band reduces the width of the valence band in $\alpha$-Pu. The predicted narrowing should be observable in photoemission experiments on $\alpha$- and $\delta$-Pu.

## I. INTRODUCTION

To date, the high-temperature fcc $\delta$ phase (stable from 583 to 725 K) is the only one of the six crystallographic allotropes of Pu that has been studied extensively within the framework of electronic structure calculations.[1–4] This phase can be stabilized as an alloy at room temperature through the addition of small amounts of Al, Ga, or Si and is known to be ductile. The experimentally observed room-temperature phase ($\alpha$-Pu) is monoclinic with 16 atoms in the unit cell, its atomic volume is some 20% smaller than that of $\delta$-Pu, and it is brittle. At $T = 388$ K $\alpha$-Pu undergoes a phase transition to the even more complicated monoclinic $\beta$ phase with 34 atoms in the unit cell.[5] The remaining solid phases are orthorhombic $\gamma$-Pu (eight atoms per unit cell), body centered tetragonal $\delta'$-Pu (two atoms per unit cell) and bcc $\epsilon$-Pu. Comparison of the rich phase diagram of Pu with that of the heavier actinides Am, Cm, Bk, Cf, and Es suggests a fundamentally different electronic structure for Pu. Whereas in the heavier actinides the $f$ electrons are invariably localized, this might not be the case in all six phases of Pu. For each of the light actinides Th, Pa, U, and Np, which have relatively dispersive $f$ bands, no more than three solid phases exist. Only $\beta$-U has a large number of atoms (30) in the unit cell, all other structures having no more than eight atoms per unit cell. This places Pu at the point of the actinide series where the transition from itinerant to atomlike $5f$ states is made.

UPS spectra of $\alpha$-Pu and $\delta$-Pu (Ref. 6) resemble each other, which may be due to the surface reconstruction of $\alpha$-Pu to a $\delta$-like surface.[7] Narrowing of the $5f$ states in $\delta$-Pu can be observed when compared with $\alpha$-Pu but no final conclusions could be drawn from these spectra. Intuitively one is tempted to link large atomic volumes for actinide metals with localized $5f$ states and predominantly $6d$ bonding, whereas $5f$ bonding is expected to become more and more important in allotropes with a lower atomic volume. The $\gamma \rightarrow \alpha$ phase transition in Ce is also accompanied by a 20% reduction in atomic volume. For this rare-earth metal it was demonstrated that the phase transition can be understood in terms of a Mott transition from localized to itinerant $4f$ states.[8,9] Perhaps bonding by $5f$ electrons might even be held responsible for the brittleness of $\alpha$-Pu, a property typically encountered in covalently bonded solids. From earlier calculations on $\delta$-Pu alloyed with Al, Ga, and Si it was found that these alloying components shift the Fermi level in such a way that $f$ bonding decreases. This decrease in $f$ bonding enhances the $d$ bonding characteristics which are also found in pure $\delta$-Pu. An argument along similar lines might also apply to the electronic structure of $\delta$-Pu when compared to $\alpha$-Pu. So far the precise nature of the $5f$ electrons in different phases of Pu, and its connection to material's properties as exhibited by the allotropes, have not been clearly established. It is therefore highly desirable to have a theoretical prediction of the electronic

 

structure of $\alpha$-Pu as well as $\delta$-Pu.

In this paper an attempt is made to gain insight into the phase stability of Pu on the basis of electronic structure calculations. The strategy is to investigate what effects can be held responsible for the relative stability of the $\alpha$ phase with respect to the $\delta$ phase and to fictitious hexagonal phases that bear some resemblance to the $\alpha$ phase. It is found that in going from fcc and hexagonal structures to $\alpha$-Pu the rearrangement of the atoms is such that $5f$ bonding becomes feasible. The $6d$ system in $\alpha$-Pu is more localized due to reduced coordination numbers. An upward shift of the bottom of the valence band is predicted and should be observable in a photoemission experiment. In Sec. II relevant details in connection with the linear muffin-tin orbital (LMTO) method employed in this work are presented. The results of electronic structure calculations for fcc and hexagonal Pu are presented in Sec. III, for monoclinic Pu in Sec. IV. Concluding remarks are gathered in Sec. V.

## II. COMPUTATIONAL METHOD

Electronic structures for $\delta$-, hexagonal (hex) and $\alpha$-Pu have been obtained from the LMTO method within the atomic (Wigner-Seitz) sphere approximation[10,11] (ASA), employing the von Barth-Hedin exchange-correlation potential.[12] For the core electrons the single-particle Dirac equation is solved.[13] Since the spin-orbit interaction is known to influence the atomic volumes of the actinides significantly,[14] the effect of spin-orbit interaction on the band states was added to the Hamiltonian as described by Koelling and Harmon.[15] In spin-polarized calculations the spin-orbit interaction was added to the Hamiltonian using the average of the spin-up and spin-down potential. In this way hermiticity of the Hamiltonian is guaranteed. The electronic structure was iterated to self-consistency for all electrons in the system.

Since the atomic $6s$ and $6p$ levels of the early actinides still have appreciable values at the Wigner-Seitz sphere radii, these states had to be treated as a semicore in a separate energy panel in order to obtain reliable energy-volume curves for $\delta$- and hex-Pu. This doubles the number of diagonalizations to be performed. For the fcc and hexagonal structures all the LMTO energy parameters were chosen at the center of the occupied partial density of states (DOS), except for the $p$-type function in the upper panel, which was kept fixed at the center of the canonical $7p$ band. Since the present study considers $\alpha$-Pu only at the experimental density corresponding to an atomic sphere radius ($S$) of $3.18a_0$, the $6s$ and $6p$ states were treated as real core states, thereby reducing the computational effort. Two-panel test calculations on $\alpha$-Pu indicated that unphysical ghost band states affect the electronic structure. The single-panel calculations carried out on $\alpha$-Pu did not suffer from this artifact.

$\alpha$-Pu can be viewed as a severely distorted hexagonal structure (Fig. 1), hence the reason for considering (nonexistent) hexagonal phases of Pu. When $\delta$-Pu is also treated as a three-atom per unit cell hexagonal structure, interesting comparisons with hexagonal Pu become feasible, provided the set of $k$ points used for $\delta$-Pu forms a subset of the $k$ points used for hex-Pu. In sampling the Brillouin zone (BZ) for hex-Pu a mesh of 112 points in the irreducible $\frac{1}{24}$th part was used to set up the $k$-space integration by the tetrahedron method.[16,17] Subsequently a properly rescaled subset of 84 of these 112 $k$ points was used in the $\delta$-Pu calculations. For $\alpha$-Pu a set of 40 $k$ points was used in the irreducible $\frac{1}{4}$th part of the monoclinic BZ.

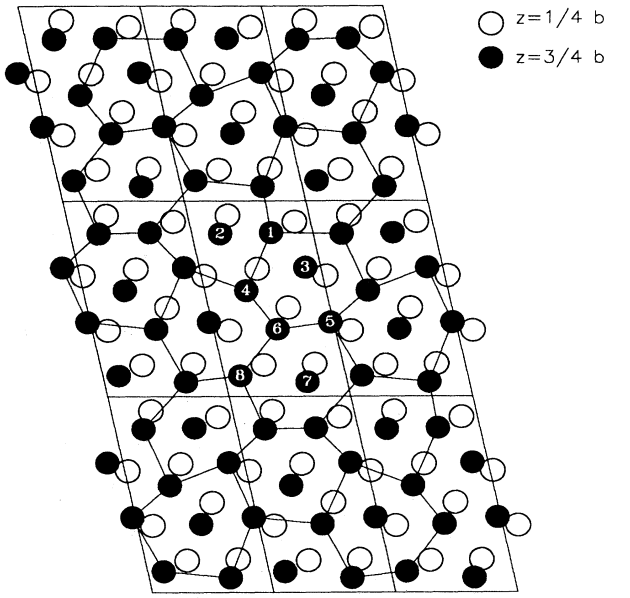


FIG. 1. A 3 × 3 array of $\alpha$-Pu unit cells viewed along the monoclinic $b$ axis. In the layer of atoms at $z = \frac{3}{4}b$ an arrangement reminiscent of a hcp structure is being suggested. The eight inequivalent atoms in this layer are numbered.

Electronic structure calculations in the ASA give reliable charges (occupation numbers) and densities of states. However, it is well known that total energies suffer from an important drawback, namely that structure dependent electrostatic contributions to the total energy are represented in an approximate way. This is most clearly illustrated by the fact that in the ASA the electrostatic energy of a hexagonal monatomic metal does not depend correctly on the $\frac{c}{a}$ ratio. Since the atomic spheres are charge neutral, only the electrostatic interaction of the nucleus with the electronic charge density inside its own atomic sphere is accounted for. The muffin-tin or Ewald correction provides a way to estimate the error involved.[18] The electrostatic energy per ion for a system of point charges in a neutralizing uniform electron gas is compared to the electrostatic energy of an ion in a single atomic sphere. This gives rise to a correction to the total energy $\Delta U_M = \frac{1.8-\alpha_M}{S}[\frac{4}{3}\pi S^3 n(S)]^2$ where $n(S)$ is the charge density at the atomic sphere radius and $\alpha_M$ is the lattice Madelung constant. This correction is expected to be most reliable for lattices that do not deviate much from close-packed structures. $\Delta U_M$ is included in all total energies for Pu quoted in this paper.

All calculations were carried out on (a cluster of) DEC

workstations. In order to obtain band-structure data for $\alpha$-Pu within a reasonable amount of time, the LMTO code was parallelized with respect to the diagonalization of the individual secular equations in different $k$ points, using the parallel virtual machine (PVM) software package.[3]

## III. $\delta$- AND HEXAGONAL PLUTONIUM

A series of calculations on $\delta$-Pu in the normal fcc structure was performed. In order to avoid complications in the BZ integration associated with spin-orbit interaction in magnetic systems, a mesh of 3375 $k$ points throughout the *whole* BZ was used. At a Wigner-Seitz radius $S = 3.20a_0$ a spin-magnetic moment develops suddenly, growing rapidly to a value of $M_S$=4.02$\mu_B$ at the experimental $\delta$-phase density ($S = 3.42a_0$). The orbital contribution ($M_L$) to the total magnetic moment, arising from spin-orbit coupling in magnetic systems, was calculated to be $M_L = -2.43\mu_B$. This results in a total magnetic moment of $1.59\mu_B$. The magnetic moments were computed along the [001] axis, other directions were not considered. In calculating $M_L$ a method outlined in Refs. 19 and 20 was followed. Figure 2 shows the ferromagnetic band structure along $Z\Gamma X$ at the experimental density. Note however that the bulk of neither pure nor impurity stabilized $\delta$-Pu is known to be magnetic experimentally.

The total-energy minimum for $\delta$-Pu occurs in the paramagnetic region, at $S = 2.98a_0$, and is in good agreement with earlier results of Wills and Eriksson.[4]

Besides cancellation of spin and orbital magnetic moments, another way of explaining the absence of a net magnetic moment in $\delta$-Pu would be to assume antiferromagnetic coupling between, for instance, [100] or [111] planes in the fcc crystal. Calculations on antiferromagnetically coupled Pu at the experimental density of the $\delta$ phase show that ferromagnetic Pu is substantially lower in total energy than both types of antiferromagnetically ordered Pu. In order to avoid the introduction of errors in subtracting total energies, ferromagnetic Pu in the abovementioned calculations were treated in the same unit cell as the antiferromagnetic structures, but with the antiferromagnetic coupling switched off. So these antiferromagnetic phases of fcc-Pu do not restore the experimentally observed absence of a net magnetic moment in Pu.

Recently Solovyev *et al.*[3] were able to obtain results for $\delta$-Pu from a fully relativistic (i.e., $\kappa\mu$ basis) LMTO calculation. They treated the noble gas core, derived from an atomic calculation on Pu ([Rn] $7s^25f^6$), as frozen.[21] Differences between their magnetic band structure and Fig. 2 can be observed and cannot simply be attributed to the frozen core but may be due to a different treatment of the spin density in $\delta$-Pu employed by Solovyev *et al.* These authors report the onset of a ferromagnetic moment at $S = 3.22a_0$, growing to $M_S$=4.5$a_0$ at the experimental density with $M_L = -2.4\mu_B$, in fair agreement with the present results. At a density corresponding to $S = 3.18a_0$ (nonmagnetic) the band-structures and DOS are nearly identical.

Figure 3 shows total energy per atom vs Wigner-Seitz sphere radius for four modifications of Pu, described in the hexagonal crystal system. These curves were obtained from LMTO calculations in which the hexagonal BZ was sampled as described in Sec. II and include the muffin-tin correction. This allows a more reliable comparison of total energies for fcc and hexagonal structures. Test calculations on hex-Pu with three different $\frac{c}{a}$ ratios but with the same atomic volume ($S$=2.93$a_0$), using additional sets of 180 and 330 $k$ points in the irreducible part of the BZ, revealed an uncertainty in the (Ewald-corrected) total-energy differences of the order of 0.1 mRy.

Ordering the curves by their minima, the upper curve

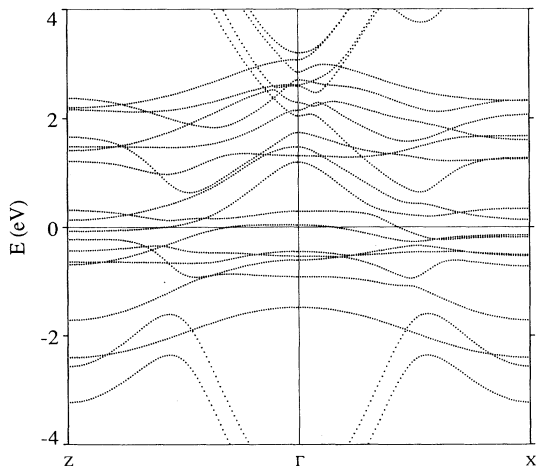


FIG. 2. Band structure of ferromagnetic $\delta$-Pu along $Z\Gamma X$. Atomic sphere radius, $S = 3.42a_0$, and the axis of spin quantization is along $\Gamma Z$. The Fermi level is at 0 eV.

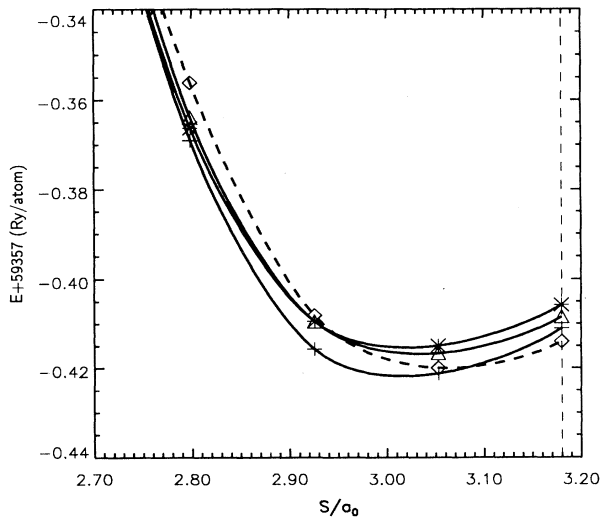


FIG. 3. Total energy per atom plus 59 357 Ryd, including the Ewald correction ($E_{\text{total}}$) vs Wigner-Seitz radius ($S$) for four modifications of Pu: $\diamond$, $\delta$-Pu; $\triangle$, hex-Pu with $\frac{c}{a} = 1.633$; $*$, $\frac{c}{a} = 1.560$; $+$, $\frac{c}{a} = 1.759$. The dashed vertical line represents the experimental $\alpha$-Pu radius.

corresponds to the hexagonal structure with $\frac{c}{a}$=1.560 while the next curve pertains to the hexagonal close-packed structure ($\frac{c}{a}$ = 1.633). Next the fcc structure has a minimum total energy which is about 4 mRy lower than that for ideal hcp-Pu. The remaining fourth curve corresponds to $\frac{c}{a}$ = 1.759 and has the deepest minimum (about 5 mRy lower than hcp-Pu). Note that at the experimental $\alpha$-Pu density ($S = 3.18a_0$) the fcc structure is found to be most stable. Further it is worthwhile mentioning that inclusion of the muffin-tin correction to the ASA did reverse the ordering of the upper three curves. Hexagonal Pu with the largest $\frac{c}{a}$ ratio ($\frac{c}{a}$=1.759) remained the structure with the lowest total-energy minimum although energy differences between the different structures were reduced.

The choices for the two nonideal $\frac{c}{a}$ ratios were directly inspired by the experimentally observed monoclinic structure of $\alpha$-Pu which, when viewed as a collection of eight two-atom "hexagonal" unit cells, gives rise to the above-mentioned extremes for $\frac{c}{a}$. Also an average $\frac{c}{a}$ ratio of 1.687 can be defined and is intermediate between the closed-packed structure and the structure with $\frac{c}{a}$=1.759. This will become even more clear in Sec. III, when the $\alpha$-Pu structure is discussed.

Equilibrium volumes per atom found for the four structures do not vary much (sphere radii between 3.0 and $3.1a_0$) and are some 12% smaller than the $\alpha$-Pu density. The total-energy curves show that hexagonal Pu can lower its energy considerably in going from the close-packed structure to a structure with a larger $\frac{c}{a}$ ratio. This leads to a more open hexagonal lattice, making the structure more similar to $\alpha$-Pu.

Figures 4(a) and 4(b) display the DOS per atom for fcc-Pu and the hexagonal structure with $\frac{c}{a}$=1.759, respectively, calculated at the experimental $\alpha$-Pu density. Both cases show a strongly dispersive $6d$ band which extends to slightly lower energies for fcc- than for hex-Pu. The $5f$ bands are of comparable width. The Fermi level, $E_F$, falls in a region where neither of the states originating from the $5f_{\frac{5}{2}}$ and $5f_{\frac{7}{2}}$ atomic levels contribute significantly to the DOS. For both structures this results in a very low DOS at the Fermi level. These observations again are in agreement with the results reported by Solovyev *et al.*

A look at the occupation numbers $n_s$, $n_p$, $n_d$, and $n_f$ for the partial DOS as function of Wigner-Seitz radius proves to be informative. Figure 5(a) shows $n_s$ and $n_p$, indicating a lower (0.01 – 0.03 electron) but otherwise similar $s$ occupation for the three hexagonal structures when compared with fcc-Pu. The $s$ occupation increases as a function of atomic volume. fcc-Pu has the overall highest $f$ occupation. Surprisingly the $f$ occupation [(Fig. 5c)] is *higher* for the two *high*-energy hexagonal structures than for the energetically most favorable hexagonal structure ($\frac{c}{a}$ = 1.759). This certainly was not to be expected from the assumption that the $5f$ electrons give the dominant contribution to the total bonding in Pu. In itself reduction of $n_f$ upon expansion of the lattice was also observed for Th, Pa, and U.[4] Among the hexagonal structures a higher occupation of the itinerant $6d$ band [Fig. 5b] correlates with a lower total-energy minimum. The fcc structure has the overall lowest $d$ occupation. Skriver[18] already pointed out that for the transition metals and the lanthanides the $d$ electron count can serve as a predictor for the crystal structure. It therefore is interesting to note that $n_d \simeq 2$ is precisely in the region where Skriver expects more complicated structures (double hcp, Samarium-type) to be lower in energy than than fcc, hcp, and bcc.

Figure 5(b) exhibits another remarkable feature, namely a maximum for the individual $n_d$ curves occurring to the left of the equilibrium sphere radii. Such an extremum in one of the $n_l$ can occur in three band sys-

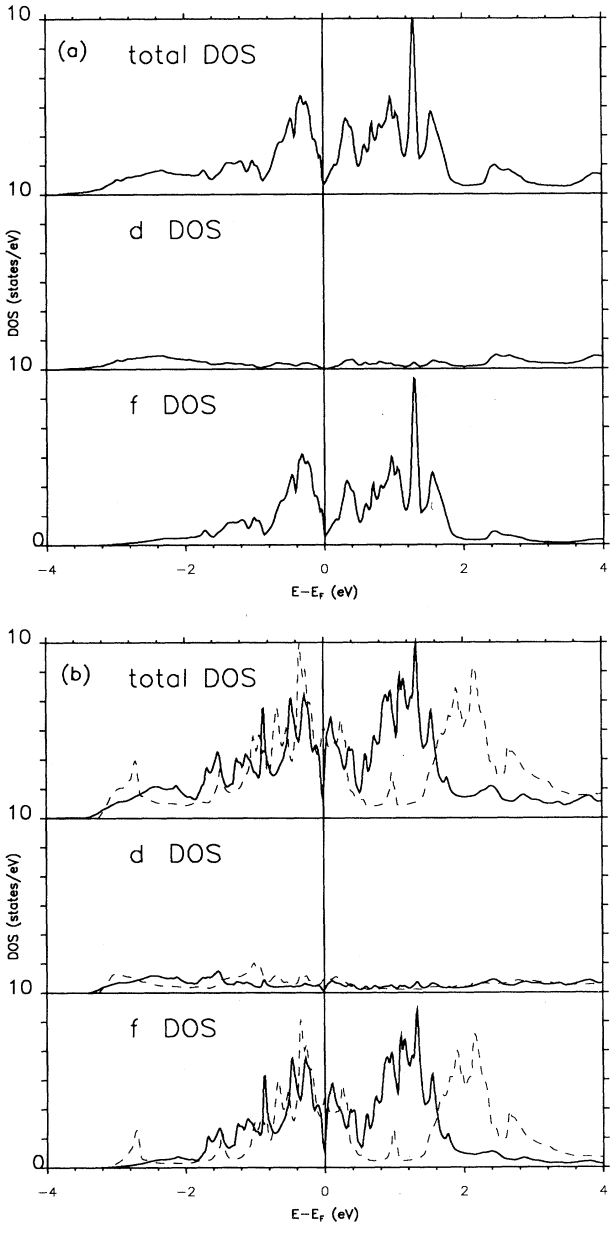


FIG. 4. Total, $d$, and $f$ density of states for (a) fcc-Pu and (b) hex-Pu at the $\alpha$-Pu density. Thick line, $\frac{c}{a}$=1.759; dashed line, $\frac{c}{a}$=2.488.

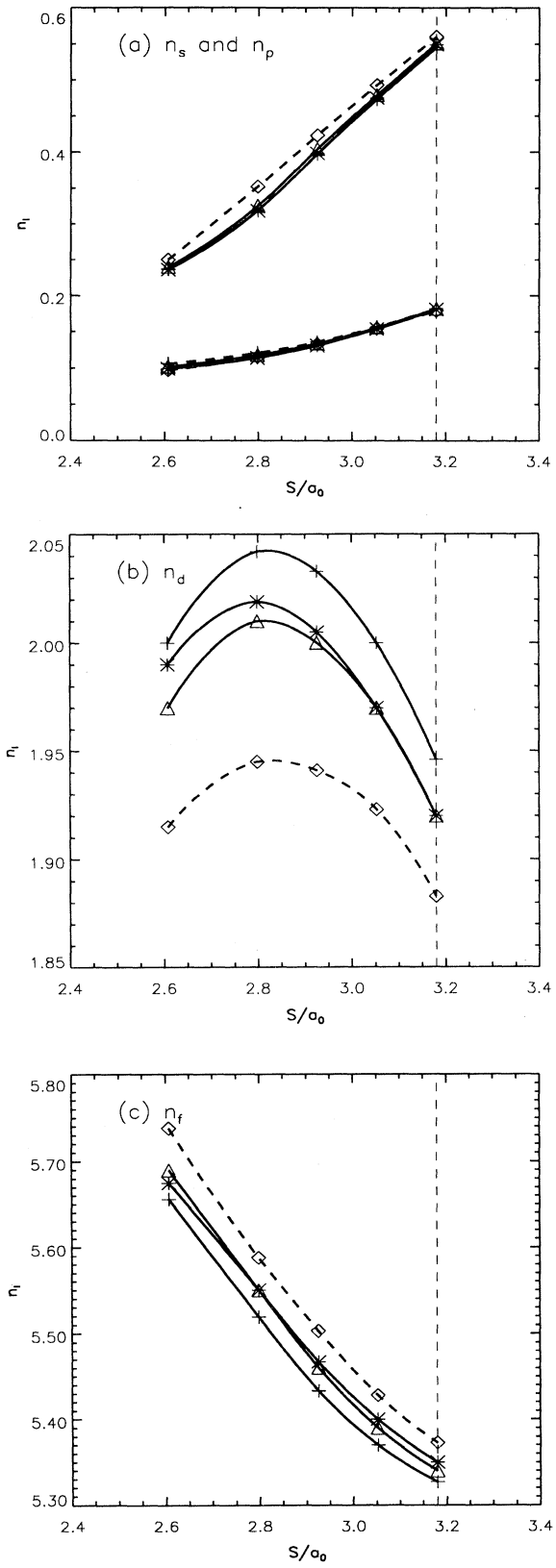


FIG. 5. Occupation numbers vs Wigner-Seitz radius ($S$) for four modifications of Pu. (a) $n_s$ (upper curves) and $n_p$, (b) $n_d$, (c) $n_f$. Symbols and dashed vertical line as in Fig. 3.

TABLE I. Wigner-Seitz radii, total energies, and occupation numbers for U in the fcc structure.

| $S$ ($a_0$) | $E_{\text{total}} + 56\,140$ (Ry/atom) | $n_s$ | $n_p$ | $n_d$ | $n_f$ |
|---|---|---|---|---|---|
| 3.020 | -0.6260 | 0.455 | 0.138 | 2.191 | 3.215 |
| 3.084 | -0.6320 | 0.491 | 0.155 | 2.203 | 3.150 |
| 3.148 | -0.6326 | 0.526 | 0.174 | 2.210 | 3.090 |
| 3.213 | -0.6290 | 0.559 | 0.193 | 2.211 | 3.037 |
| 3.341 | -0.6120 | 0.618 | 0.231 | 2.199 | 2.952 |

tems where the occupation numbers do not vary strictly linearly with the atomic sphere radius.

The above-mentioned observations express a tendency towards maximizing the occupation of the itinerant $6d$ band in highly coordinated hexagonal Pu. However for fcc-Pu, which is the structure second lowest in energy, promotion of a fraction of the $d$ electrons to the $s$ and $f$ bands is observed when compared to hex-Pu.

At this point it is worthwhile to make a brief excursion to another actinide metal, U, which is generally believed to be an itinerant $5f$ electron system.[22] Accurate total-energy calculations for fcc-U, based on a full-cell LMTO method, already exist.[4] In order to compare with the calculations of Ref. 4, a large number of $k$ points (220) was used in the $\frac{1}{48}$th irreducible wedge of the fcc BZ. From a series of calculations (see Table I) the equilibrium Wigner-Seitz radius was estimated to be $S = 3.13a_0$, in agreement with the result for fcc-U, as obtained by Wills and Eriksson ($S \simeq 3.14a_0$).[4] Inspection of the partial occupation numbers in Table I again show an, albeit shallow, maximum in $n_d$. Note that the $d$ occupation numbers reported here are about one electron higher than those cited in Ref. 4, which is due to the fact that in Ref. 4 only those electrons inside the muffin-tin sphere are being counted. However, a substantial fraction of the itinerant $d$ electrons is likely to be found in the interstitial region, which may account for the absence of a maximum in $n_d$ in the results of Wills and Eriksson.

As stated clearly in Ref. 4 the overall highest $5f$ occupation, as found for the experimentally observed, more open $\alpha$-U structure, can be linked intuitively to the delocalized and therefore more bonding character of $5f$ electrons in U. In Pu this correlation with $5f$ occupation seems to be lost as far as fcc and hexagonal structures are concerned. Instead $6d$ bonding becomes more important, while the $5f$ electrons are beginning to localize.

Proceeding from energetically unfavorable hexagonal structures to a more open, nonideal hexagonal structure with a larger $\frac{c}{a}$ ratio which is lower in energy, a final perturbation of the lattice leads to Pu in its low-temperature $\alpha$-phase.

## IV. $\alpha$-PLUTONIUM

The structure of $\alpha$-Pu at $T$=294 K was described by Zachariasen and Ellinger[23] and consists of a 16-atom monoclinic unit cell ($a$=11.684$a_0$, $b$=9.112$a_0$, $c$=20.717$a_0$, $\beta$=101.79°) with eight pairs of equivalent atoms. The space group is $C_{2h}^2$ ($P2_1/m$) with the atoms placed in special positions ($2e$),[24] indicating that the lattice has inversion symmetry. Equal atomic volumes for

all 16 atoms implies a Wigner-Seitz radius of $S = 3.18a_0$. Figure 1 shows an array of 3 × 3 unit cells and indicates an hexagonal arrangement. Interpreting one monoclinic unit cell as a collection of 4 × 2 ordinary two-atom hexagonal cells, one readily arrives at the two extremes for the hexagonal $\frac{c}{a}$ ratios ($\frac{4b}{c} = 1.759$, $\frac{2b}{a} = 1.560$) considered in the previous section. The average $\frac{c}{a}$ ratio, defined as $\frac{6b}{c+a}$=1.687, is slightly larger than for the hcp structure and would be a fourth option but is not considered here.

In a further analysis of the $\alpha$-Pu structure Zachariasen and Ellinger distinguish short bonds (range $4.86 - 5.25a_0$) and long bonds ($6.03 - 7.01a_0$) from individual Pu atoms to their neighbors. Table II summarizes their results. In addition, information on close-packed structures at the $\alpha$-Pu atomic volume is given. Although strictly speaking the nonideal hexagonal structures have a 6+6 coordination, the interatomic distances differ only slightly from those for the ideal 12-fold coordinated hcp structure.

Since LMTO calculations for $\alpha$-Pu are extremely time consuming, only results at the experimental density are presented here. The calculation of the energy-volume curve for $\alpha$-Pu, including treatment of the $6s/6p$ semicore in a separate energy panel, will be the subject of future research.

The total DOS for $\alpha$-Pu [(Fig. 6a)] is different from the DOS for the fcc and hexagonal structures in the following respects. First, due to the low symmetry of the $\alpha$ phase many degeneracies of electronic states are lifted. In addition to that the total DOS consists of a superposition of the DOS for the eight inequivalent atoms. This accounts for the structureless appearance of the DOS. As a direct consequence of this large number of inequivalent atoms the minimum in the DOS around $E_F$, which can be observed in fcc and hex-Pu at $S = 3.18a_0$, has disappeared completely. Extrapolation[3] of the low DOS at $E_F$ found for fcc-Pu at the experimental $\alpha$ density, to the DOS of true monoclinic $\alpha$-Pu must therefore be deemed meaningless. Second, the valence band has a steep onset at 2.8 eV below the Fermi energy, whereas in fcc and hex-Pu the DOS per atom reaches appreciable values at 3.5 eV below $E_F$. Such a narrowing of the valence band suggests a relative lowering of the $f$ band in $\alpha$-Pu. It should be possible to observe this upward shift of the bottom of the valence band in a photoemission experiment.

Figure 6(b) shows the contribution to the DOS from the different types of atoms and Table III summarizes the occupation numbers and atomic charges for the eight types of atoms in $\alpha$-Pu. In order to be able to compare with $\delta$- and hex-Pu, results from single-panel calculations on these systems are included in Table III. Minimal changes in the occupation numbers (in the order of 2–5 %) are found from comparison of single- and two-panel calculations. The relative ordering of the different structures with respect to occupation numbers is identical to that obtained from the two-panel calculations. DOS from the two types of calculations do not differ noticeably. However, the relative ordering of the Pu struc-

TABLE II. Short bonds ($4.86 - 5.25a_0$) and long bonds ($6.03 - 7.01a_0$) in $\alpha$-Pu for the eight different types of atoms. The third column gives the average short bond length. For comparison the close-packed value is shown in the bottom row.

| Atom | Number of short bonds | Average short bond length | Number of long bonds |
|---|---|---|---|
| 1 | 5 | 5.01 | 7 |
| 2 | 4 | 4.95 | 10 |
| 3 | 4 | 4.97 | 10 |
| 4 | 4 | 5.05 | 10 |
| 5 | 4 | 5.01 | 10 |
| 6 | 4 | 5.12 | 10 |
| 7 | 4 | 5.03 | 10 |
| 8 | 3 | 5.23 | 13 |
| Close packed | 12 | 5.75 | - |

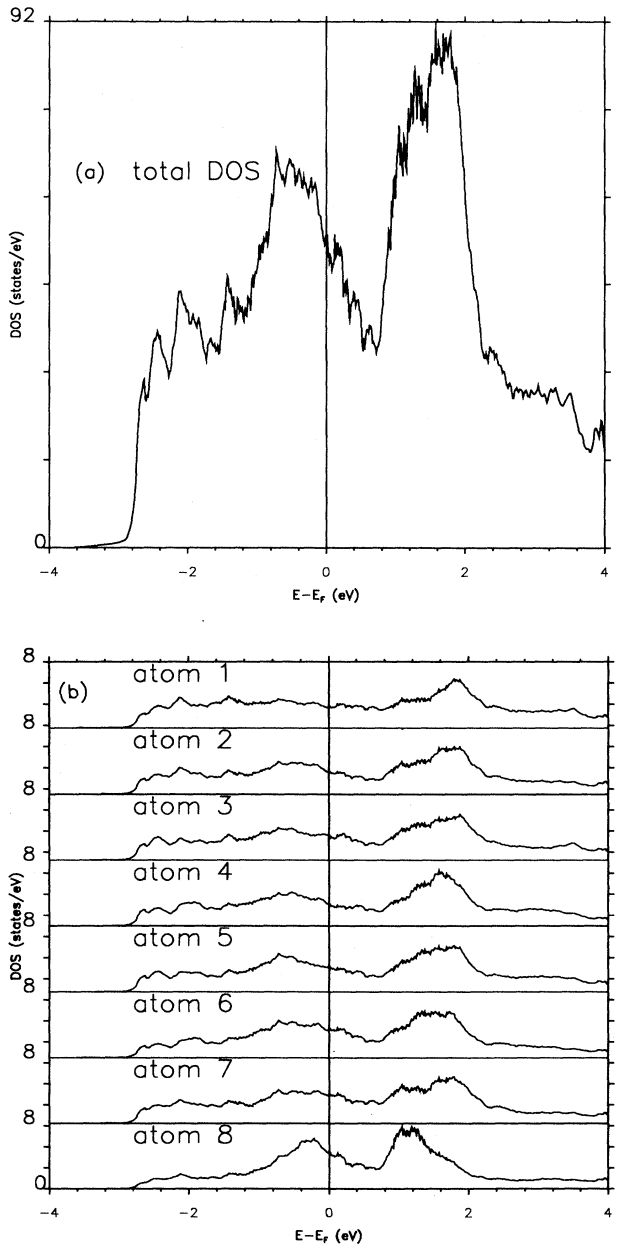


FIG. 6. (a) Total DOS for $\alpha$-Pu, (b) DOS per atom in $\alpha$-Pu.

TABLE III. Occupation numbers, total electron count per atomic sphere and total energies, including the Ewald correction, for $\delta$-, hex-, and $\alpha$-Pu at $\alpha$ density. Results from single-panel LMTO calculations.

| Structure | | $n_s$ | $n_p$ | $n_d$ | $n_f$ | $n_{\text{total}}$ | $E_{\text{total}} + 59\,357$ (Ry/atom) |
|---|---|---|---|---|---|---|---|
| fcc | | 0.573 | 0.194 | 1.967 | 5.267 | 8 | -0.9477 |
| hex | $\frac{c}{a}$=1.560 | 0.563 | 0.195 | 2.009 | 5.232 | 8 | -0.9421 |
| hex | $\frac{c}{a}$=1.633 | 0.566 | 0.197 | 2.012 | 5.225 | 8 | -0.9418 |
| hex | $\frac{c}{a}$=1.759 | 0.569 | 0.197 | 2.037 | 5.207 | 8 | -0.9536 |
| $\alpha$ | On average | 0.428 | 0.167 | 2.178 | 5.227 | 8 | -1.0482 |
| Atom | 1 | 0.469 | 0.159 | 2.534 | 5.321 | 8.483 | |
| | 2 | 0.416 | 0.160 | 2.240 | 5.254 | 8.071 | |
| | 3 | 0.404 | 0.177 | 2.246 | 5.206 | 8.034 | |
| | 4 | 0.433 | 0.174 | 2.183 | 5.247 | 8.037 | |
| | 5 | 0.426 | 0.169 | 2.207 | 5.231 | 8.033 | |
| | 6 | 0.424 | 0.165 | 2.050 | 5.168 | 7.808 | |
| | 7 | 0.416 | 0.180 | 2.225 | 5.207 | 8.029 | |
| | 8 | 0.435 | 0.148 | 1.741 | 5.183 | 7.506 | |

tures according to their total energy at $S = 3.18a_0$ has changed. From the single-panel calculations the ordering, increasing with energy, is found to be $\frac{c}{a}$=1.759, fcc, $\frac{c}{a}$=1.560, $\frac{c}{a}$=1.633. This is a consequence of the inadequate description of the $6s/6p$ semicore in Pu by single-panel LMTO calculations. The main purpose of these single-panel calculations is to compare occupation numbers with those obtained for $\alpha$-Pu and to detect a large energy difference between $\alpha$-Pu and the fcc and hexagonal modifications of Pu.

What immediately leaps to the eye in Table III are the $s$ and $d$ occupation numbers in $\alpha$-Pu. On average $n_s$=0.428 is smaller than the smallest value for either $\delta$- or hex-Pu. The average $d$ occupation $\langle n_d \rangle = 2.178$ is larger than the largest value, whereas $\langle n_f \rangle$ is comparable to the values for $\delta$- and hexagonal Pu. This means that with respect to the simple structures a substantial $s$ to $d$ charge transfer of about 0.15 electrons takes place in $\alpha$-Pu. Further inspection of Table III in combination with Table II shows that atom 1 has by far the highest $n_d$ and total number of electrons ($n_{\text{total}}$) together with the maximum number of short bonds. Atom 8 has the combination of the lowest $n_d$, lowest $n_{\text{total}}$, and only 3 short bonds. Atom 6 resembles atom 8 (low $n_d$, $n_{\text{total}}$) while the other atoms (2, 3, 4, 5, 7) are similar with respect to $n_d$, $n_{\text{total}}$, number of short bonds and DOS [(Fig. 6b)]. The classification of the different types of atoms on the basis of geometrical considerations according to Zachariasen and Ellinger is clearly reflected by $s$ and $d$ occupation numbers, $n_{\text{total}}$ and partial densities of states obtained from a band-structure calculation.

In Fig. 7 the total and partial $d$ and $f$ DOS for three different types of atoms (1, 5, 8) in $\alpha$-Pu are shown. Here atom 5 has been chosen to represent a larger group of atoms with similar characteristics (bonds and DOS). Note the sharp transition metal-like onset of the $d$ DOS (atoms 1 and 5) contrary to the more itinerant character found for the $d$ band in fcc/hex-Pu and atom 8. With the exception of atom 8, all $\alpha$-Pu atoms have a region of relatively high $d$ DOS at the bottom of the valence band. Apart from an upward shift of the bottom of the very itinerant $7s$ band, its shape remains more or less unaffected by the fcc/hex to $\alpha$ transition. This means that due to an increased $d$ DOS at low energies an appreciable $s$ to $d$ charge transfer can take place. Going from atom 1 to 5 to 8 to fcc/hex the $d$ band flattens while the $f$ band narrows. The $f$ band width for atom 8 and fcc/hex Pu are comparable, whereas all other atoms in $\alpha$-Pu have a wider $f$ band.

The above observations can be explained by assuming that the number of short bonds determines the $f$ band width while the total number of long *and* short bonds influences the itinerancy of the $d$ electrons. This is consistent with a different range of the radial wave function for the $d$ and $f$ electrons. Reduction of the number of nearest neighbors from 12 to about 4 reduces the itinerancy of the $d$ electrons. Longer bonds ($6.03 - 7.01a_0$) will restore the itinerant character of the $d$ band, but only to a certain extent since the bond lengths are much larger than for the closed-packed structures (see Table II).

In the highly coordinated fcc and hexagonal structures the nearest-neighbor atoms are relatively far away (see Table II), prohibiting strong overlap between $5f$ states on adjacent atoms. However, the number of and distance to neighboring atoms guarantees the existence of itinerant $7s$ and $6d$ bands. Differences in lattice geometry between fcc and various hexagonal structures merely change the occupation of the partial bands but are not able to alter the overlap between $5f$ states on different sites significantly. Increasing $5f$ overlap in these highly coordinated structures through a simple reduction of the lattice constant is prohibited by the (12-fold) nuclear repulsion term in the total energy.

In going from an hexagonal lattice to the $\alpha$-Pu structure the atoms do undergo a rearrangement by which the number of shortest bonds is reduced from 12 to about 4 and, along with that, the average length of the short bonds is reduced considerably (9–14 %). This redistribution of the internuclear potential energy allows for considerable lowering of the total energy through $5f$ bonding. All Pu atoms in the unit cell engage in $f$ bonding with three to five neighboring atoms. An increase in the num-

ber of short (or $f$) bonds is reflected in a wider $f$ DOS for the different types of atoms in $\alpha$-Pu. The empirical observation that brittleness of actinides correlates with $f$ bonding and ductility with $d$ bonding,[25] is confirmed in the particular case of Pu.

In order to investigate the differences between the $d$ DOS as found for the different types of atoms in $\alpha$-Pu, an additional calculation on an hexagonal structure with $\frac{c}{a}=2.488$ was carried out. At this $\frac{c}{a}$ ratio the distance to the six nearest neighbors is $5.00a_0$, close to the average short bond length of atom 1 in $\alpha$-Pu. Compared to the three hexagonal structures that were discussed in Sec. III an $s$ to $d$ charge transfer of about 0.15 is found, similar to the average $s$ to $d$ charge transfer in $\alpha$-Pu. The DOS for the elongated hexagonal system is shown as a dashed line in Fig. 4(b). Notice the widening of the $f$ band due to an increased overlap between $f$ states on sixfold coordinated atoms in the [0001] planes. At low energies an increase in the $d$ DOS along with a relative upward shift is observed, very similar to what was found for most of the atoms in $\alpha$-Pu. The increase and upward shift have their origin in a reduced overlap between the $d$ orbitals on atoms in different [0001] planes. These bonding states of reduced itinerancy have become less favorable in energy relative to the $f$ band. An $s$ to $d$ charge transfer takes place in states at the bottom of the valence band since the $7s$ band is strongly hybridized with the $6d$ band but much less affected by an increase of the $\frac{c}{a}$ ratio.

Although the separation between the planes in $\alpha$-Pu is not as large as in the elongated hexagonal struc-

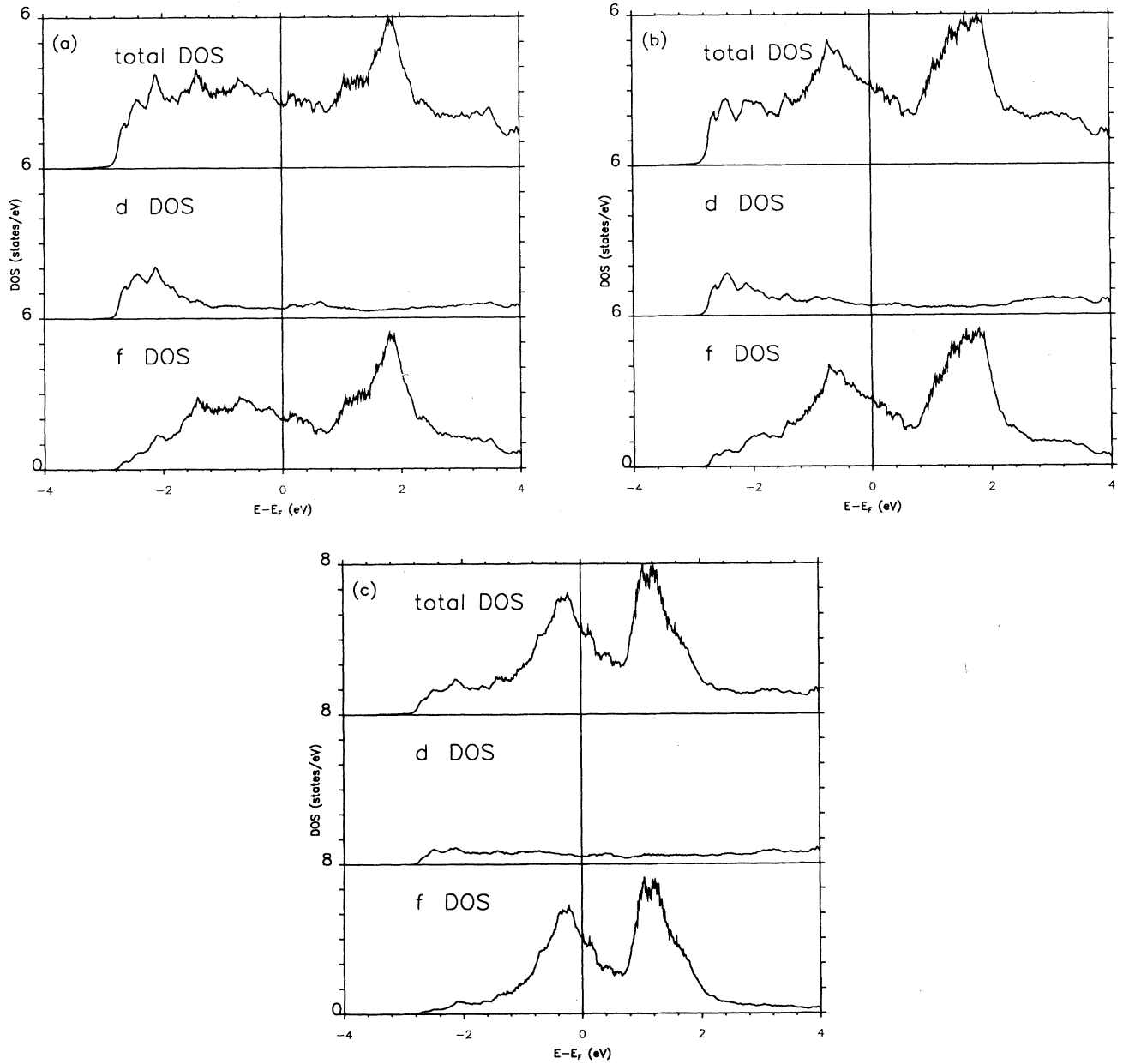


FIG. 7. Total, $s$ and $d$ partial DOS for atoms (a) 1, (b) 5, and (c) 8 in $\alpha$-Pu.

ture, a correlation between the character of the atom-decomposed $d$ DOS and its surroundings can be established. Atom 1 has a total of 12 bonds (see Table II) of which 7 are about $6.5a_0$ long. These seven distant atoms are unable to restore the itinerancy of the $d$ electrons completely for they are few and far away. Atom 8, on the other hand, has 3 short bonds and 13 long bonds. This large number of surrounding atoms is able to restore the more delocalized nature of the $d$ electrons to some extent. Restoration of $d$ itinerancy implies a lower $d$ electron count because the Fermi level is pinned by the $f$ band. This is reflected by the $n_d$ for atoms 1 to 8 in Table III.

The very low total energy for $\alpha$-Pu in Table III might tempt one to conclude immediately that $\alpha$-Pu is the most stable of the five structures considered. This cannot be justified rigorously since no convergence of the total energy with respect to the number of $k$ points in the calculation was attained yet. As explained in Sec. II only total energies for fcc and hexagonal Pu structures can be compared directly. Since it is desirable to obtain an impression of the relative stability of $\alpha$-Pu when compared to fcc/hex-Pu, a procedure described by Skriver[18] is adopted here. Skriver applied his method successfully in predicting the lattice structure at zero temperature for many metals. For an elemental metal Skriver's method in essence amounts to a direct comparison of the sum of the valence one-electron energies and the structure dependent muffin-tin or Ewald correction for different lattice structures. The all-electron electronic structure for a reference system, here the one atom-per-unit-cell fcc structure, is taken to self-consistency in the sense that the sum of the one-electron energies have converged to the desired level of accuracy (0.1 mRy). This required 4950 $k$ points in the irreducible part of the fcc BZ. Next the frozen potential from the fcc calculation is used to calculate one-electron energy sums for other structures. Cancellation of the core and double counting contributions to the total-energy difference between two structures is guaranteed. Structural energy differences obtained in this way were shown to be useful in predicting low-temperature lattice structures,[18] provided the one-electron energy sums have converged with respect to the number of $k$ points used in the calculation.

Results of such calculations (single energy panel) for fcc-, hexagonal and $\alpha$-Pu are gathered in Table IV. Convergence of the one-electron energy sums is slow, and accuracy in the 0.1 mRy range is attained only at high $k$-point densities. The relative stability for the fcc and hexagonal structures ($S = 3.18a_0$) is in agreement with that obtained from fully self-consistent single-panel calculations, i.e., in order of decreasing energy $\frac{c}{a}$=1.633, $\frac{c}{a}$=1.560, fcc, and $\frac{c}{a}$=1.759. The average energy sum for the $\alpha$-Pu atoms in Table IV is about 0.15 Ry lower than those for fcc and hex-Pu and is composed of a one-electron part of $-0.723$ Ry and an Ewald correction of 0.327 Ry. Since the Ewald correction to the ASA is of the same order of magnitude as the one-electron sum its accuracy in the case of an open structure like $\alpha$-Pu (average Madelung constant $\langle\alpha_M\rangle = 1.766\,143$) can be questioned. Nevertheless it is unlikely that an error of more than 0.15 Ry is involved.

## V. CONCLUSIONS

Electronic structure calculations on Pu in 12-fold coordinated fcc and hexagonal structures show an overall picture of a metal with a strongly itinerant $6d$ band and a much more localized $5f$ band. Widening of the $f$ band in $\alpha$-Pu is attributed to the formation of a low number of short bonds thereby reducing the itinerancy of the $d$ band. In $\alpha$-Pu the valence band narrows about 0.7 eV due to a downward relative shift of the $f$ band. This effect should be observable in a photoemission experiment.

The stability of the three hexagonal structures around their energy minimum was found to correlate with *higher* $d$- and *lower* $f$-band occupations. The hexagonal structure with a $\frac{c}{a}$ ratio larger than the ideal $\frac{c}{a}$ ratio was found to be most stable, followed by the fcc structure, the hexagonal closed-packed structure, and hex-Pu with $\frac{c}{a}$=1.560. Equilibrium atomic sphere radii are calculated to lie between 3.0 and $3.1a_0$, smaller than the experimental $\alpha$-Pu sphere radius. At the experimental $\alpha$-Pu density a pronounced minimum in the DOS around $E_F$ was observed for both the fcc and hexagonal structures.

For fcc-Pu at the experimental $\delta$-Pu density a spin plus orbital magnetic moment of $4.02-2.43=1.59\mu_B$ was found, whereas from the experimental point of view no magnetic moment was to be expected. Antiferromagnetically ordered forms of $\delta$-Pu were found to be higher in energy than ferromagnetic Pu, so the absence of ferromagnetism in experiment cannot be explained readily in terms of more complicated magnetic orderings.

At the experimental density the low-temperature $\alpha$ phase of Pu was shown to be the one lowest in energy

TABLE IV. Sums of one-electron energies and Ewald correction (Ry/atom) as a function of the density of $k$ points in the Brillouin zone. fcc-Pu ($S = 3.18a_0$) is the reference system (see text).

| Volume per $k$ point ($10^{-5}a_0{}^{-3}$) | fcc (hex system) | hex ($\frac{c}{a}$=1.560) | hex ($\frac{c}{a}$=1.633) | hex ($\frac{c}{a}$=1.759) | $\alpha$ (average) |
|---|---|---|---|---|---|
| 71.933 | | | | | -0.39696 |
| 19.982 | | | | | -0.39647 |
| 1.662 | -0.24012 | | | | |
| 1.829 | | -0.23508 | -0.23472 | -0.24868 | |
| 0.919 | -0.24014 | | | | |
| 0.908 | | -0.23510 | -0.23474 | -0.24870 | |

of the five structures considered in this work. Of the eight pairs of equivalent atoms in $\alpha$-Pu the DOS of only one pair resembles that found for fcc or hex-Pu. All other atoms in the $\alpha$-Pu unit cell contribute a $d$ DOS with a transition-metal-like onset at low energies and a more delocalized $f$ DOS to the featureless total density of states of $\alpha$-Pu. Pu atoms that most resemble fcc- and hex-Pu account for 7.5 electrons per atom while those with the highest $d$ DOS at low energies and the broadest $f$ band have 8.5 electrons per atomic sphere. The number of short bonds per atom was found to be a measure of the width of the atom-decomposed $f$ band, whereas the total number of short and long bonds determines the itinerancy of the atom decomposed $d$ DOS.

In summary this means that Pu strives to maximize bonding by $5f$ electrons. The formation of a low symmetry structure allows normally excluded overlap between $5f$ states on neighboring atoms. Of 12 bonds to nearest neighbor atoms in fcc and hex-Pu only $3-5$ bonds at shorter distances remain in $\alpha$-Pu. The itinerancy of the $d$ electrons is reduced as a consequence of this atomic rearrangement in which the majority of the nearest-neighbor atoms is displaced to substantially larger distances. Depending on the number of long bonds the delocalized character of the $d$ electrons is partially recovered. The structure still profits as much as possible from the more localized $6d$ states via a substantial $7s$ to $6d$ charge transfer at energies near the bottom of the $d$ band, where the $d$ density of states has increased relative to the $s$ density of states.

Significant differences in the electronic structure between close-packed and monoclinic Pu demonstrate that $\alpha$-Pu cannot be appropriately modeled by either fcc or hexagonal Pu. In these highly coordinated structures nuclear repulsion does not allow the atoms to approach each other close enough for the formation of $f$ bonds. Bonding in the close-packed crystals involves primarily $s$ and $d$ electrons but in $\alpha$-Pu a significant admixture of $f$ bonding is found. For Pu the empirical rule that $d$ bonding results in ductility ($\delta$ phase) and $f$ bonding in brittleness ($\alpha$ phase) holds.

## ACKNOWLEDGMENT

This work was performed under the auspices of the U.S. Department of Energy by Lawrence Livermore National Laboratory under Contract No. W-7405-ENG-48.

[1] P. Weinberger, A. Gonis, A.J. Freeman, and A.M. Boring, Physica **B130**, 13 (1985).
[2] H.L. Skriver, B. Johansson, and O.K. Andersen, Phys. Rev. Lett. **41**, 42 (1978).
[3] I.V. Solovyev, A.I. Liechtenstein, V.A. Gubanov, V.P. Antropov, and O.K. Andersen, Phys. Rev. B **43**, 14414 (1991).
[4] J.M. Wills and O. Eriksson, Phys. Rev. B **45**, 13879 (1992).
[5] *Landolt-Börnstein, New Series*, Vol **19**f1 (Springer, Berlin, 1991).
[6] J.R. Naegele (unpublished).
[7] O. Eriksson, L.E. Cox, B.R. Cooper, J.M. Wills, G.W. Fernando, Y.G. Hao, and A.M. Boring, Phys. Rev. B **46**, 13 576 (1992).
[8] B. Johansson, Philos. Mag. **30**, 469 (1974).
[9] O. Eriksson, M.S.S. Brooks, and B. Johansson, Phys. Rev. B **41**, 7311 (1990).
[10] O.K. Andersen, Phys. Rev. B **12**, 3060 (1975).
[11] H.L. Skriver, *The LMTO Method* (Springer, Berlin, 1984).
[12] U. von Barth and L. Hedin, J. Phys. C **5**, 1629 (1972).
[13] J.P. Desclaux, C.M. Moser, and G. Verhaegen, J. Phys. B **4**, 296 (1971).
[14] M.S.S. Brooks, J. Phys. F **13**, 103 (1983).
[15] D.D. Koelling and B.N. Harmon, J. Phys. C **10**, 3107 (1977).
[16] O. Jepsen and O.K. Andersen, Solid State Commun. **9**, 1763 (1971).
[17] G. Lehman and M. Taut, Phys. Status Solidi B **54**, 469 (1972).
[18] H.L. Skriver, Phys. Rev. B **31**, 1909 (1985).
[19] M. Singh, J. Callaway, and C.S. Wang, Phys. Rev. B **14**, 1214 (1976).
[20] M.S.S. Brooks and P.J. Kelly, Phys Rev. Lett. **51**, 1708 (1983).
[21] A.I. Liechtenstein (private communication).
[22] A.J. Freeman and D.D. Koelling, in *The Actinides: Electronic Structure and Related Properties,* (Academic, New York, 1974), Vol. 1.
[23] W.H. Zachariasen and F.H. Ellinger, Acta Crystallogr. **16**, 777 (1963).
[24] R.W.G. Wyckoff, *Crystal Structures* (Interscience, New York, 1966).
[25] C.E. Olsen (private communication).